GMDH-based 3-D Reactor Power Reconstruction for Increment of Operation Margin of MDNBR Calculation in Core Monitoring System

Dongmin Yun, Deokjung Lee*
Department of Nuclear Engineering, Ulsan National Institute of Science & Technology, 50 UNIST-gil, Ulsan, 44919
**Corresponding author: deokjung@unist.ac.kr*

1. Introduction

The Core Operating Limits Supervisory System (COLSS) is an important component of commercial reactor core monitoring systems (CMS), developed by Combustion Engineering, Inc. [1]. It collects reactor coolant measurements and in-core neutron detector signals and calculates multiple core safety parameters in real-time. The COLSS conservatively calculates lumped one-dimensional axial power distribution and multiplies penalties to estimate safety parameter.

This study aims to model the machine learning algorithm that synthesize the 3-D Assembly Power Distribution (APD) from in-core detector data, then increase the margin of the most critical safety parameter of the CMS, the minimum Departure from Nucleate Boiling Ratio (MDNBR), by replacing the conservative penalty with model uncertainty. The General Method of Data Handling (GMDH), which was developed by Ivakhnenko [2], is used for the regression model. GMDH has the merits of model-transparency, low memory usage, and high accuracy to perform on the on-line COLSS environment. The training data for GMDH are produced using 3-D whole-core two step code STREAM/RAST-K, which has been developed in UNIST [3].

The methods and results of each procedure, including input data acquisition, GMDH training, and uncertainty evaluation, have been explained. Two GMDH models have been developed: one for the 3-D assembly power distribution and the other for the hot-pin's power distribution (HPD). This paper also explains various ways to apply these regression models on the COLSS to increase the operational margin of MDNBR.

2. Methods and Results

This section explained that the procedure of 1-D APD model of original COLSS and 3-D APD reconstruction using GMDH model pre-trained with data from STREAM/RAST-K, which are applied to MDNBR calculation in COLSS monitoring. By replacing the 1-D APD in original COLSS as the 3-D APD reconstruction model GMDH, the conservative penalties from 1-D model can be also replaced as the uncertainty of GMDH model.

2.1 APD and DNBR in COLSS

The model of 1-D axial power distribution consists of the Fourier spline fitting with radially averaged 5-level detector power and two boundary conditions [4]. This model utilizes only the averaged information of detector power and loses the other radially distributed information. COLSS multiplies the highly conservative penalty factors on the fitted distribution to calculate the maximum APD for the next step of DNBR algorithm.

The MDNBR is defined as the ratio of the critical heat flux to the local heat flux, which is regarded as the hot-pin heat flux (HHF) for the MDNBR value. The critical heat flux (CHF, q''_{chf}) and MDNBR can be expressed as:

$$q''_{chf} = \dot{m} h_{fg} (T_{sat} - T_{sub}) \tag{1}$$

$$MDNBR = \frac{q''_{chf}}{q''_{hot-pin} \times F_v} \tag{2}$$

$$F_v = \frac{Q_{actual}}{q''_{uniform} \times area} \tag{3}$$

, where $\dot{m}$ is the mass flow rate, h_{fg} is the enthalpy of evaporation, T_{sat} is saturation temperature and T_{sub} is subcooled temperature. The non-uniform flux correction factor (F_v) is defined as the ratio of the actual heat transfer rate to the heat transfer rate that would occur if the heat flux were uniform.

2.2 GMDH 3-D Power Reconstruction

The input data of the 3-D model are the 5 detector powers from 45 In-core instrumentation assemblies (ICI). To optimize data utilization for training GMDH, the input batch consists of the power readings from 20 detectors located in four ICIs adjacent to each target assembly. The target data consists of 3-D APD shapes for 177 assemblies and 40 axial nodes, and 1-D hot-pin power distribution.

The data are acquired by the whole-core calculation of STREAM/RAST-K, at the 60% ~ 100% core power, and randomly inserted control rod following power dependent insertion limit (PDIL) from the selected core power. In a dataset, 40,000 data are split by 32,000 (80%) of training, 4,000 (10%) of validation, and 4,000 (10%).

The models are trained with the self-organizing multi-layered iterative algorithm (MIA) that provides linear polynomial regression [5]. The Ivakhnenko polynomial which is the basis function of GMDH model is [2]:

$$p_{i,j} = a_0 + a_1 x_i + a_2 x_j + a_3 x_i^2 + a_4 x_i x_j + a_5 x_j^2 \tag{4}$$

, where i and j are the data selection index from the input batch. At the first layer of MIA, ${}_{20}C_2$ (= 190) polynomials and those coefficients are computed with least square. The set of 50 polynomials, ranked by their smallest loss value using the L1 Loss function, is forwarded to the next layer. The maximum number of layers is 20, but the layer forward is stopped when model is overfitted.

The evaluation metric of GMDH model accuracy is relative difference (RD, %) between the value from GMDH and RAST-K:

$$RD_{xy,z} = \frac{P_{GMDH,xy,z} - P_{RAST-K,xy,z}}{P_{RAST-K,xy,z}} \times 100\% \qquad (5)$$

The following Fig. 1. ~ Fig. 4. show the results of 3-D APD reconstruction and 1-D HPD reconstruction, comparing them to those of RAST-K.

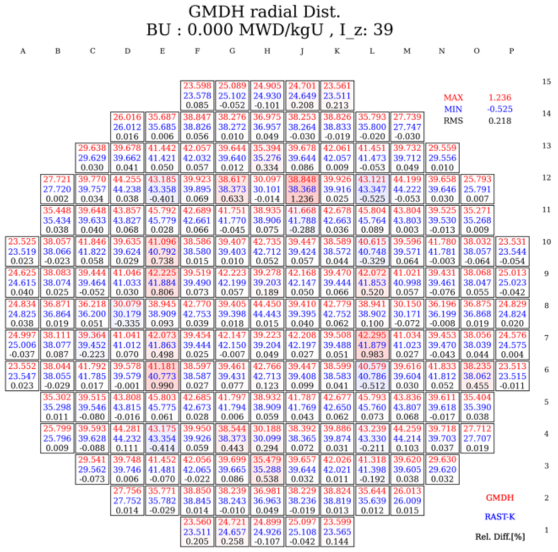

Fig. 1. The radial assembly power distribution of GMDH and RAST-K, top node of the OPR-1000 BOC core (unit: W/cm^3).

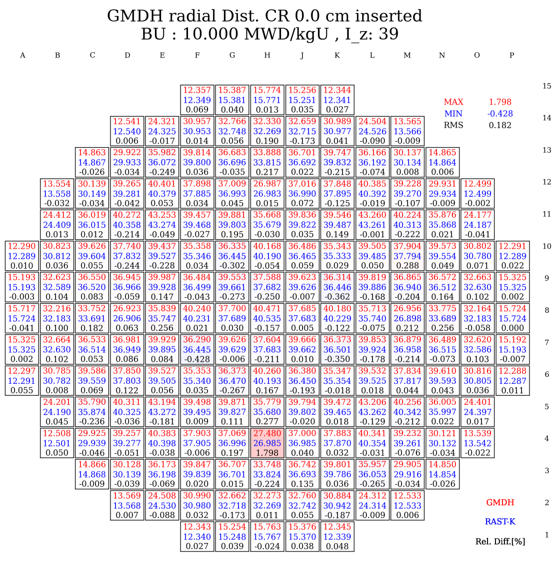

Fig. 2. The radial assembly power distribution of GMDH and RAST-K, top node of the OPR-1000 MOC core (unit: W/cm^3).

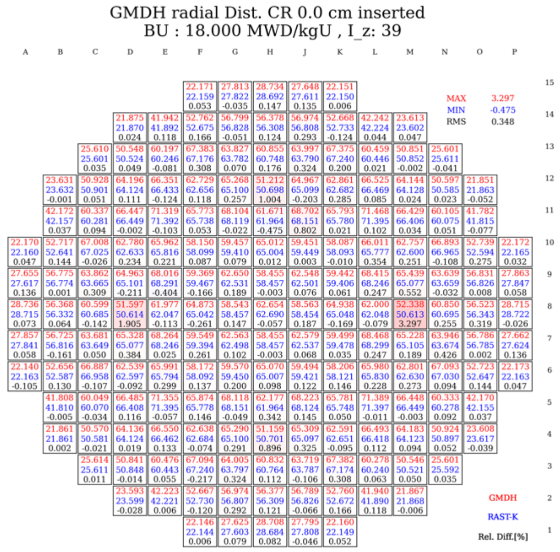

Fig. 3. The radial assembly power distribution of GMDH and RAST-K, top node of the OPR-1000 EOC core (unit: W/cm^3).

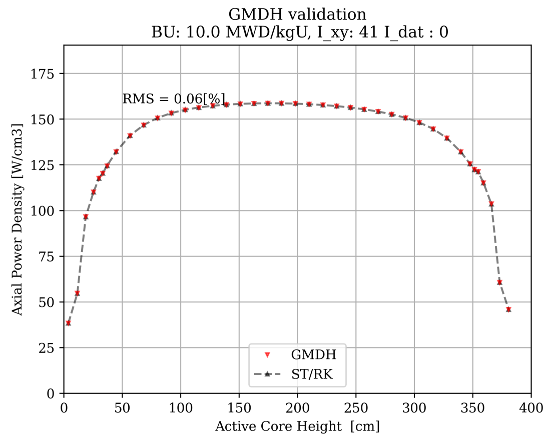

Fig. 4. The axial hot-pin power distribution of GMDH and RAST-K, OPR-1000 MOC core.

It is shown that the RD of R5 control rod installed positions are up to around 3%, and the other APD are accurately fit. The root mean squared (RMS) of RD are 0.218%, 0.182%, and 0.348% for BOC, MOC, and EOC top node of core.

2.3 Uncertainty Evaluation of GMDH Model

To apply the GMDH model on the COLSS, the model uncertainty should be evaluated and applied for final results. Fig. 5. Shows the 3-D RD histogram of (4,000 test data × 177 assemblies × 40 axial nodes) test dataset of RAST-K and predicted values of GMDH model. The normality test of the trained model by the histogram shape and the Shapiro-Wilk normality test failed then the uncertainty evaluation can be implemented by non-parametric uncertainty analysis methods.

The X% of confidence limit (CL) α and β are obtained from the numerical of probability density function $p(x)$:

$$\int_{\alpha<x<\beta} p(x)dx = X(=0.99) \quad (5)$$

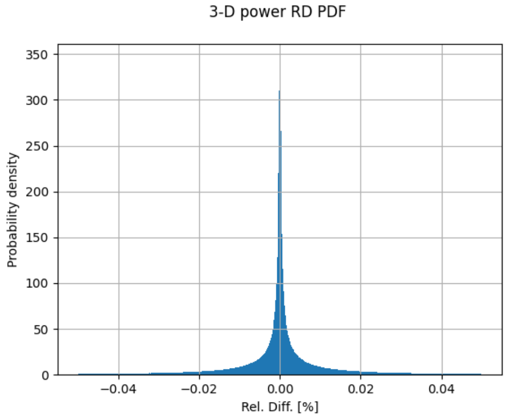

Fig. 5. The probability density function of RD for GMDH trained model (p-value of Shapiro-Wilk test = 0.001)

Table I. shows the 99% confidence limit obtained from the one of available non-parametric uncertainty analysis methods, bootstrapping [6]. $GMDH_a$ refers to the model trained for the 3-D APD, while $GMDH_b$ refers to the model trained for the 1-D HPD.

Table I: 99% confidence limits for GMDH model RD (%).

Synthesis Model	Lower limit (α)	Upper Limit (β)
3-D APD	-0.3889	0.3505
1-D HPD	-0.6593	0.7438

Through this process, the propagation of uncertainty in the calculation of DNBR using COLSS can be evaluated. When applying GMDH models to COLSS, the uncertainties of the models propagate through several modules in COLSS. We have conducted an uncertainty analysis using a sampled test dataset and the uncertainty of the predicted values from GMDH can propagate to those of the MDNBR results.

2.4 COLSS Application for DNBR safety margin

Recalling Eq. (1), the critical heat flux (q''_{chf}) is derived from temperature and enthalpy changes with respect to the 1-D axial power distribution obtained from Fourier spline fitting, multiplied by the control-rod penalty factor, planar peaking factor, and integrated radial peaking factor (INTRAD). However, we now have a 3-D APD and a 1-D HPD that enable COLSS to eliminate the INTRAD in the original lumped model. That significantly reduces the critical heat flux, which is the denominator of DNBR calculation.

The following cases are implemented to compare the original COLSS and GMDH applied COLSS. Table II. describe whether GMDH model applied for each module. Spline fitting and TH calculation are the equivalent methods to original module. Table III. results the operation margins of MDNBR and corresponding CHF and HHF value which are multiplied 99% confidence limits. The results show elimination of penalties by using 3-D estimation especially increases the CHF values. The tabulated MDNBR results are picked from the most conservative value, which is the minimum among the 10,000 perturbed values of GMDH predictions. The values in parentheses represent the nominal values of MDNBR, which assume that the GMDH models are accurate.

Table II: Application of Method Case Description

Case	APD	HPD
1	$GMDH_a$	$GMDH_b$
2	$GMDH_a$	TH calculation
3	Spline fitting	$GMDH_b$
4 (ref.)	Spline fitting	TH calculation

Table III: Uncertainty adjusted DNBR operation margin
(The results in parenthesis are nominal values)

Case	Minimum MDNBR	Margin changed. From case 4., [%]	CHF	HHF
			[BTU/ft^2-sec]	
1	2.3150 (2.3457)	13.10 (14.60)	250.39 (250.18)	107.38 (105.03)
2	2.2983 (2.3163)	12.29 (13.17)	244.13 (244.58)	104.15 (103.53)
3	1.9434 (1.9686)	-5.05 (-3.82)	204.93 (196.30)	101.47 (100.28)
4	2.0468	-	187.43	84.40

The following Fig. 6. shows the axial results of DNBR distribution with respect to the method application cases. Fig. 7. shows HHF distribution along the axial core height. The case 1 and 3 use the $GMDH_b$ model for synthesizing 1-D HPD that is directly converted to same HHF results. The HHF of case 2 is derived from APD of GMDH, while that of case 4 is derived from the APD of Spline fitting and the shape skewness is corrected. The case 1 and 2 use the $GMDH_a$ model for APD, but case 3 and 4 use the Fourier spline fitting model for APD. Fig. 7. shows the distribution of CHF values derived solely from the APD.

Referring to the HHF results in Fig. 7., the original HHF calculation method produces axially symmetric tuning from the top-skewed detector power input. However, the flux level itself is not much affected from the 3-D method. Otherwise, Fig. 8. shows that eliminating the penalty from the evaporation enthalpy change (h_{fg} in Eq. (1)) significantly increases the CHF at the top of the core. These CHF increments obviously lead to DNBR margin increments.

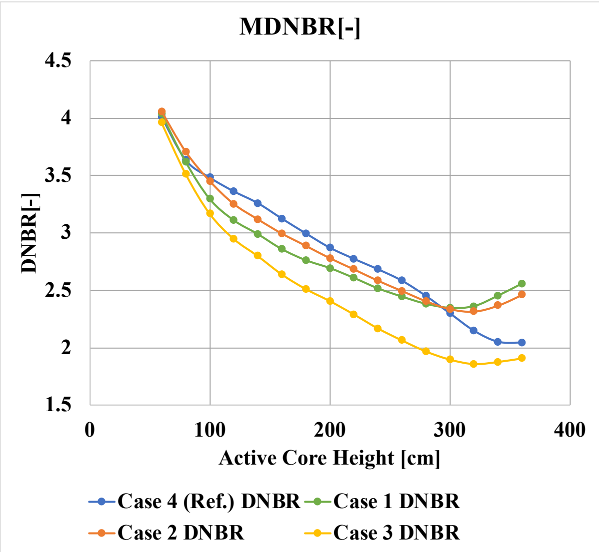

Fig. 6. Axial MDNBR distribution of GMDH applied COLSS.

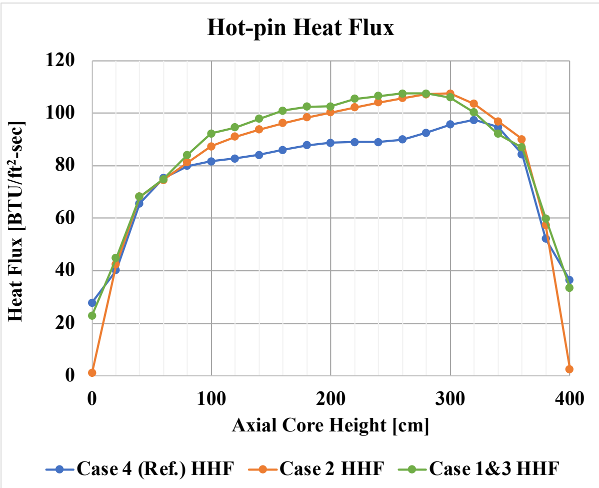

Fig. 7. Hot-pin Heat Flux distribution of GMDH applied COLSS (unit: BTU/ft^2-sec).

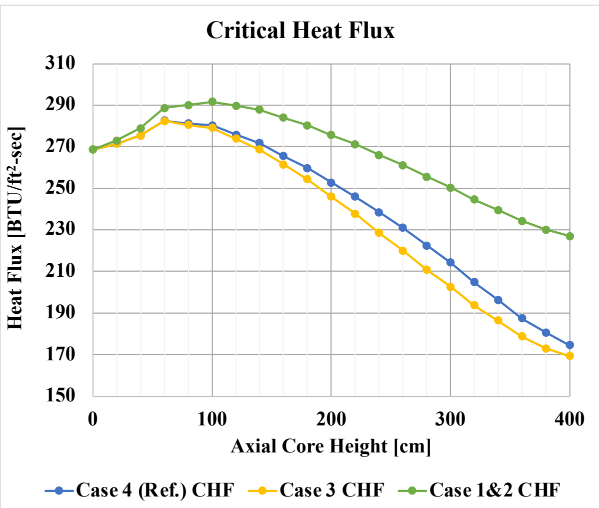

Fig. 8. Critical Heat Flux distribution of GMDH applied COLSS (unit: BTU/ft^2-sec).

Table IV: Calculation resources of COLSS with GMDH (Processor/OS: Intel Core i7 2.3GHz, macOS 13.0.1)

Resources	COLSS	COLSS with GMDH
Data reading time [ms]	20~25	1300
Calculation time [ms]	1 ~ 2	5~10
Memory [MB]	1.6	16~ 17

Table IV shows the calculation resources required for GMDH applied in COLSS and as a stand-alone method. The reading of the model from the GMDH coefficient DB takes a few seconds, but this only occurs at the beginning of the surveillance process. The calculation time and memory usage are quite practical for use in the main control room devices currently in use.

3. Conclusions

The GMDH method can be used for 3-D power reconstruction and monitoring safety margins. In Case 1, where separate GMDH models were used, the operational margin for DNBR increased by 15.01%. However, there are internal and epistemic uncertainties in the application of both the COLSS module and GMDH module, such as ensuring appropriate usage of coefficients. Other safety parameters such as ASI, Azimuthal Tilt, and LHR values are not significantly affected by using the 3-D method since they are global values. When replacing penalty values with 3-D uncertainty values, the effects of eliminating other factors should be studied more thoroughly through the derivation of those penalties.

This study aims to apply a training-based model to a real-time core monitoring system. Unlike the original monitoring system, the GMDH input data does not require exact knowledge of the positions of control rods. The innovative Small Modular Reactor (i-SMR) operates with freely moving control rods, making the exact position of the rods uncertain. The ICI detector-power-based model could be an attractive alternative for monitoring the i-SMR. The power synthesis GMDH model for i-SMR core has broader domain to solve due to various positions of control rod induced power shifts. To train GMDH for those skewed power shape, the order of polynomial would be higher and the number of GMDH layer increased.

4. Acknowledgement

This study was sponsored by the Korea Hydro & Nuclear Power Co.'s affiliated Central Research Institute (KHNP-CRI).

REFERENCES

[1] Combustion Engineering, Inc., Overview Description of the Core Operating Limit Supervisory System (COLSS), CEN-312-NP, Rev. 01-NP, 1986.
[2] Ivakhnenko, A.G., The Group Method of Data Handling – a Rival of the Method of Stochastic Approximation, Soviet Automatic Control Journal, 13, 43-55, 1968.
[3] Jiwon Choe, Sooyoung Choi, Peng Zhang, Jinsu Park, Wonkyeong Kim, Ho Cheol Shin, Hwan Soo Lee, Ji-Eun Jung, Deokjung Lee*, "Verification and validation of STREAM/RAST-K for PWR analysis," Nuclear Engineering and Technology, ISSN 1738-5733, https://doi.org/10.1016/j.net.2018.10.004, 2018.
[4] Moon-Ghu Park, Generation of Optimal Basis Functions for Reconstruction of Power Distribution, Transactions of the Korean Nuclear Society Spring Meeting, 2014.
[5] Tetyana I. Aksyonova, ROBUST POLYNOMIAL NEURAL NETWORKS IN QUANTATIVE-STRUCTURE ACTIVITY RELATIONSHIP STUDIES, Systems Analysis Modelling Simulation, Vol. 43, No. 10, pp.1331-1339, 2003.
[6] Barmak Mostofian, Error Analysis for Small-Sample, High-Variance Data: Cautions for Bootstrapping and Bayesian Bootstrapping, Biophysical Journal, Volume 116, Issue 3, Supplement 1, pp. 140a, ISSN 0006-3495, https://doi.org/10.1016/j.bpj.2018.11.779., 2019.